JOURNAL OF GUIDANCE, CONTROL, AND DYNAMICS
Vol. 30, No. 1, January–February 2007

Hubble Space Telescope Angular Velocity Estimation During the Robotic Servicing Mission

Julie K. Thienel*
NASA Goddard Space Flight Center, Greenbelt, Maryland 20771
and
Robert M. Sanner†
University of Maryland, College Park, Maryland 20742

DOI: 10.2514/1.20591

In 2004 NASA began investigation of a robotic servicing mission for the Hubble Space Telescope. Such a mission would require estimates of the Hubble Space Telescope attitude and rates to achieve a capture by the proposed Hubble Robotic Vehicle. The Hubble Robotic Vehicle was to be equipped with vision-based sensors, capable of estimating the relative attitude between the Hubble Space Telescope and the Hubble Robotic Vehicle. The inertial Hubble Space Telescope attitude is derived from the measured relative attitude and the Hubble Robotic Vehicle computed inertial attitude. However, the relative rate between the Hubble Space Telescope and Hubble Robotic Vehicle cannot be measured directly. Therefore, the Hubble Space Telescope rate with respect to inertial space is not known. A nonlinear approach is developed to estimate the Hubble Space Telescope rates through an estimation of the inertial angular momentum. The development includes an analysis of the estimator stability given errors in the measured attitude. Simulation test results are given, including scenarios with erroneous measured attitudes. Even though the development began as an application for the Hubble Space Telescope robotic servicing mission, the method presented is applicable to any rendezvous–capture mission involving a noncooperative target spacecraft.

I. Introduction

THE Hubble Space Telescope (HST) was launched in 1990 and has undergone four servicing missions throughout its mission lifetime to replace instruments, sensors, solar arrays, power units, and cooling systems. Additional servicing will again be necessary to extend the HST's science life. The batteries are predicted to fail as early as 2009, and the pointing control system may be reduced to a two-gyro mode by as early as 2007. On 12 March 2004 former NASA Administrator Sean O'Keefe asked the HST program to investigate robotic servicing of the HST to extend the science life. In addition to replacing the batteries and gyros, the servicing mission would install two new instruments and would provide the ability to safely deorbit the HST.

The original robotic servicing mission concept included two vehicles, a deorbit module (DM) and an ejection module (EM) with the robotic arm for servicing. The DM docks with the HST and provides batteries and gyros for the stacked HST–DM configuration. The DM also provides the reentry capability for the stacked configuration. The EM carries the robotic arm for servicing, as well as the replacement instruments. Following the servicing, the EM separates from the HST–DM stack and safely deorbits. An alternative concept to the robotic servicing mission was to provide a deorbit-only capability for the HST. A modified DM docks with the HST and provides for a safe reentry of the HST. In this work we refer to the vehicle docking with the HST as the Hubble Robotic Vehicle (HRV).

For the HRV to dock with the HST, the HRV must match the rotation rates of the HST. If either the batteries or gyros fail, the HST will be tumbling with unknown rates. The HRV will be equipped with sensors capable of estimating the relative attitude between the HST and HRV. The sensors use vision and feature-recognition measurements to produce a relative quaternion. The HRV will also be equipped with star cameras and gyros that will provide the inertial orientation and body rates of the HRV. Combining the relative attitude and HRV inertial attitude provides a measurement of the HST attitude. However, the relative rates or HST body rates cannot be measured directly.

We present a nonlinear method for estimating the HST body rates in the event that the HST is tumbling and no a priori rate information is available. Salcudean [1] presents a nonlinear method for estimating the angular velocity in body coordinates, but must rely on a simplifying assumption to verify stability. Vik et al [2] also present a nonlinear angular velocity estimator which is essentially a nonlinear estimator for gyro calibration parameters. All the error terms are modeled as exponentially decaying, first-order equations. The nonlinear approach presented in this work is built on the nonlinear gyro bias estimator presented in [3,4]. Here the HST rate is estimated through an estimation of the inertial angular momentum. The stability properties of the estimator are addressed first for perfect attitude measurements. Errors are then introduced into the HST measured attitude. The primary error source considered is the uncertainty in the relative attitude quaternion provided by the vision and feature-recognition sensors.

Even though this work was originally developed for the HST–HRV scenario, it can easily be applied to other "noncooperative" rendezvous–capture scenarios. A noncooperative scenario is one in which the body rates of the target vehicle are not available, and the target vehicle does not carry any devices to improve the relative attitude estimation, such as reflectors or visible beacons.

The paper is outlined as follows. The next section presents definitions and mathematical background. Section III presents the nonlinear estimation algorithm. Section IV discusses how

Presented as Paper 6396 at the AIAA Guidance, Navigation, and Control Conference, San Francisco, CA, 15–18 August 2005; received 17 October 2005; revision received 10 April 2006; accepted for publication 13 April 2006.

*Aerospace Engineer, Flight Dynamics Analysis Branch; currently Professor of Aerospace Engineering, Aerospace Engineering Department, U.S. Naval Academy; thienel@usna.edu. AIAA Member.

†Professor of Aerospace Engineering, Aerospace Engineering Department; rmsanner@eng.umd.edu. AIAA member.

measurement errors affect the nonlinear algorithm. Section V includes results, followed by conclusions in the last section.

II. Attitude and Angular Rate Definitions

The attitude of a spacecraft relative to a specified inertial reference is represented by a quaternion, composed from a unit vector $\boldsymbol{e}$, known as the Euler axis, and a rotation ϕ about this axis to form [5]

$$\boldsymbol{q} = \begin{bmatrix} \boldsymbol{e}\sin\left(\frac{\phi}{2}\right) \\ \cos\left(\frac{\phi}{2}\right) \end{bmatrix} = \begin{bmatrix} \boldsymbol{\varepsilon} \\ \eta \end{bmatrix} \tag{1}$$

where $\boldsymbol{q}$ is the quaternion, partitioned into a vector part $\boldsymbol{\varepsilon}$ and a scalar part η. In the following discussion, the HST attitude quaternion is designated as $\boldsymbol{q}_v$, while the HRV attitude quaternion is designated as $\boldsymbol{q}_h$.

The relative rotation between two orientations with quaternion representations $\boldsymbol{q}_1$ and $\boldsymbol{q}_2$, respectively, is [6]

$$\tilde{\boldsymbol{q}} = \begin{bmatrix} \tilde{\boldsymbol{\varepsilon}} \\ \tilde{\eta} \end{bmatrix} = \boldsymbol{q} \otimes \boldsymbol{q}_2^{-1} = \begin{bmatrix} \eta_2 I - S(\boldsymbol{\varepsilon}_2) & -\boldsymbol{\varepsilon}_2 \\ \boldsymbol{\varepsilon}_2^T & \eta_2 \end{bmatrix} \begin{bmatrix} \boldsymbol{\varepsilon}_1 \\ \eta_1 \end{bmatrix} \tag{2}$$

Thus, for example, the relative orientation between the HRV and HST is given by

$$\boldsymbol{q}_r = \boldsymbol{q}_v \otimes \boldsymbol{q}_h^{-1} \tag{3}$$

For each quaternion there is a corresponding rotation matrix, formed as [5]

$$R = R(\boldsymbol{q}) = (\eta^2 - \boldsymbol{\varepsilon}^T\boldsymbol{\varepsilon})I_3 + 2\boldsymbol{\varepsilon}\boldsymbol{\varepsilon}^T - 2\eta S(\boldsymbol{\varepsilon}) \tag{4}$$

where I_3 is a 3×3 identity matrix and $S(\boldsymbol{\varepsilon})$ is matrix representation of the vector cross product operation.

$$S(\boldsymbol{\varepsilon}) = \begin{bmatrix} 0 & -\varepsilon_z & \varepsilon_y \\ \varepsilon_z & 0 & -\varepsilon_x \\ -\varepsilon_y & \varepsilon_x & 0 \end{bmatrix}$$

Note that $R(\boldsymbol{q})\boldsymbol{\varepsilon} = \boldsymbol{\varepsilon}$, and hence $\boldsymbol{\varepsilon}$ is an eigenvector of R.

The rotation matrix for the HST is denoted $R_v = R(\boldsymbol{q}_v)$, whereas that of the HRV is $R_h = R(\boldsymbol{q}_h)$. The relative orientation between the two vehicles is then $R_r = R(\boldsymbol{q}_r) = R(\boldsymbol{q}_v)R(\boldsymbol{q}_h)^{-T}$, and the matrix R_r can be employed to express, in the HRV coordinates, quantities measured in the HST frame, or vice versa. For example, let $\boldsymbol{\omega}_v$ denote the angular velocity of the HST with respect to inertial space, measured in the HST body coordinates, and let $\boldsymbol{\omega}_h$ similarly denote the angular velocity of the HRV measured in the HRV coordinates. Then, the angular velocity of the HST relative to the HRV, given in the HST body coordinates, is given as

$$\boldsymbol{\omega}_r^v = \boldsymbol{\omega}_v - R_r\boldsymbol{\omega}_h \tag{5}$$

Finally, the time evolution of the quaternion is related to the angular velocity using the kinematic equation:

$$\dot{\boldsymbol{q}}(t) = Q[\boldsymbol{q}(t)]\boldsymbol{\omega}(t) \tag{6}$$

where

$$Q(\boldsymbol{q}) = \begin{bmatrix} \eta I_3 + S(\boldsymbol{\varepsilon}) \\ -\boldsymbol{\varepsilon}^T \end{bmatrix} = \begin{bmatrix} Q_1(\boldsymbol{q}) \\ -\boldsymbol{\varepsilon}^T \end{bmatrix} \tag{7}$$

where, by inspection, $Q_1(\boldsymbol{q}) = \eta I_3 + S(\boldsymbol{\varepsilon})$. The corresponding kinematic equation for the associated rotation matrix is [7]

$$\dot{R}(t) = -S[\boldsymbol{\omega}(t)]R(t) \tag{8}$$

III. HST Nonlinear Angular Velocity Estimator

The following angular velocity estimator is intended for the scenario in which the HST batteries have died and thus no telemetry is available from the HST. The HRV is assumed equipped with a quaternion star tracker, which gives $\boldsymbol{q}_h$, and a sensor system capable of measuring the relative orientation $\boldsymbol{q}_r$. Because from the preceding

$$\boldsymbol{q}_v = \boldsymbol{q}_r \otimes \boldsymbol{q}_h \tag{9}$$

(and hence also $R_v = R_rR_h$), the orientation of the HST can be directly determined, but not its angular velocity $\boldsymbol{\omega}_v$. The purpose of the estimator therefore is to use the available information, together with the known equations of motion, to determine the HST angular velocity. In this section, all measurements are assumed perfect; the effect of noisy measurements is considered in the next section. Note that the following analysis will suppress the time argument of all functions for brevity; it is understood that all quantities examined next are evolving continuously in time.

The angular momentum of the HST, measured in inertial coordinates, is $\boldsymbol{h}_{i,v} = I_{i,v}\boldsymbol{\omega}_{i,v}$, where $I_{i,v} = R_v^T I_v R_v$ and I_v is the constant HST inertia matrix, and where $\boldsymbol{\omega}_{i,v} = R_v^T\boldsymbol{\omega}_v$ and $\boldsymbol{\omega}_v$ is the HST angular velocity as described in the previous section. This quantity evolves in time according to [1]

$$\dot{\boldsymbol{h}}_{i,v} = T_{i,v} \tag{10}$$

where $T_{i,v}$ is the external torque acting on the HST, resolved in inertial coordinates. In the next development, $T_{i,v}$ is either assumed to be known or computable from the available measurements as described in the following section.

The evolution of the HST orientation can be expressed in terms of its angular momentum as

$$\dot{\boldsymbol{q}}_v = \tfrac{1}{2}Q(\boldsymbol{q}_v)\boldsymbol{\omega}_v = \tfrac{1}{2}Q(\boldsymbol{q}_v)R_v\boldsymbol{\omega}_{i,v} = \tfrac{1}{2}Q(\boldsymbol{q}_v)I_v^{-1}R_v\boldsymbol{h}_{i,v} \tag{11}$$

Because the actual angular momentum cannot be measured, let $\hat{\boldsymbol{h}}_{i,v}$ be an estimate of this quantity. To attempt to generate a sequence of estimates converging to the true momentum, the following strategy is used, similar to the approaches in [2,3]: propagate the HST quaternion using the current angular momentum estimate; compare this estimate to the actual measured HST orientation, and use the discrepancy between the measured and propagated attitude to adjust the angular momentum estimate. Note that the corresponding angular velocity estimate at any stage in this process can be obtained as $\hat{\boldsymbol{\omega}}_v = I_v^{-1}R_v\hat{\boldsymbol{h}}_{i,v}$.

Denote the propagated HST quaternion by

$$\hat{\boldsymbol{q}}_v = \begin{bmatrix} \hat{\boldsymbol{\varepsilon}}_v \\ \hat{\eta}_v \end{bmatrix}$$

The discrepancy between the propagated and measured orientation at any time is then

$$\tilde{\boldsymbol{q}}_v = \begin{bmatrix} \tilde{\boldsymbol{\varepsilon}}_v \\ \tilde{\eta}_v \end{bmatrix} = \boldsymbol{q}_v \otimes \hat{\boldsymbol{q}}_v^{-1} \tag{12}$$

Employing the estimator structures in [1,3,4] suggests the following equations for attitude propagation and momentum estimate adjustment:

$$\dot{\hat{\boldsymbol{q}}}_v = \tfrac{1}{2}Q(\hat{\boldsymbol{q}}_v)R(\tilde{\boldsymbol{q}}_v)^T\left[I_v^{-1}R_v\hat{\boldsymbol{h}}_{i,v} + k\tilde{\boldsymbol{\varepsilon}}_v\,\mathrm{sign}\,(\tilde{\eta}_v)\right] \tag{13}$$

$$\dot{\hat{\boldsymbol{h}}}_{i,v} = T_{i,v} + \tfrac{\alpha}{2}R_v^T I_v^{-1}\tilde{\boldsymbol{\varepsilon}}_v\,\mathrm{sign}\,(\tilde{\eta}_v) \tag{14}$$

where gains k and α can be any positive constant.

Using the preceding example, the evolution of the attitude propagation and momentum estimation errors can be computed as

$$\dot{\tilde{\boldsymbol{q}}}_v = \frac{1}{2}\begin{bmatrix} Q_1(\tilde{\boldsymbol{q}}_v) \\ -\tilde{\boldsymbol{\varepsilon}}_v^T \end{bmatrix}\left[I_v^{-1}R_v\boldsymbol{h}_{i,v} - I_v^{-1}R_v\hat{\boldsymbol{h}}_{i,v} - k\tilde{\boldsymbol{\varepsilon}}_v\,\mathrm{sign}\,(\tilde{\eta}_v)\right] \tag{15}$$

and

$$\dot{\tilde{\boldsymbol{h}}}_{i,v} = -\tfrac{\alpha}{2} R_v^T I_v^{-1} \tilde{\boldsymbol{\varepsilon}}_v \operatorname{sign}(\tilde{\eta}_v) \tag{16}$$

where $\tilde{\boldsymbol{h}}_{i,v} = \boldsymbol{h}_{i,v} - \hat{\boldsymbol{h}}_{i,v}$. Note that the equilibrium states for (15) and (16) are

$$\begin{bmatrix} \tilde{\boldsymbol{q}}_v^T & \tilde{\boldsymbol{h}}_{i,v}^T \end{bmatrix} = \begin{bmatrix} 0 & 0 & 0 & \pm 1 & 0 & 0 & 0 \end{bmatrix}$$

To prove the stability of this nonlinear estimation algorithm, consider the following Lyapunov function candidate:

$$V(t) = \frac{1}{2\alpha} \tilde{\boldsymbol{h}}_{i,v}^T \tilde{\boldsymbol{h}}_{i,v} + \frac{1}{2} \begin{cases} (\tilde{\eta}_v - 1)^2 + \tilde{\boldsymbol{\varepsilon}}_v^T \tilde{\boldsymbol{\varepsilon}}_v & \tilde{\eta}_v \geq 0 \\ (\tilde{\eta}_v + 1)^2 + \tilde{\boldsymbol{\varepsilon}}_v^T \tilde{\boldsymbol{\varepsilon}}_v & \tilde{\eta}_v < 0 \end{cases}$$

Note that V is continuous at $\tilde{\eta}_v = 0$ and that its derivative is given as

$$\dot{V}(t) = -\tfrac{k}{2} \tilde{\boldsymbol{\varepsilon}}_v^T \tilde{\boldsymbol{\varepsilon}}_v \tag{17}$$

This establishes that $\tilde{\boldsymbol{h}}_{i,v}$, $\tilde{\boldsymbol{\varepsilon}}_v$, and $\tilde{\eta}_v$ are all globally, uniformly bounded. The derivative of $\dot{V}(t)$ is

$$\ddot{V}(t) = -\tfrac{k}{2} \tilde{\boldsymbol{\varepsilon}}_v^T Q_1(\tilde{\boldsymbol{q}}_v) \left[I_v^{-1} R_v \tilde{\boldsymbol{h}}_{i,v} - k \tilde{\boldsymbol{\varepsilon}}_v \operatorname{sign}(\tilde{\eta}_v) \right]$$

which is bounded. Barbalat's lemma then shows that $\|\tilde{\boldsymbol{\varepsilon}}\| \to 0$ as $t \to \infty$ [8] (see also pages 125–126 of [9]).

Although the stability of the estimator is thus demonstrated, the real concern is the convergence of the estimation error $\tilde{\boldsymbol{h}}_{i,v}$ to zero, which has not yet been established. To demonstrate this property, note that because all signals in the estimator are bounded, the system (15) and (16) can be equivalently analyzed as [10,11] $\dot{\boldsymbol{x}}(t) = A(t)\boldsymbol{x}(t)$, where

$$\boldsymbol{x}(t) = \begin{bmatrix} \tilde{\boldsymbol{\varepsilon}}_v \\ \tilde{\boldsymbol{h}}_{i,v} \end{bmatrix} \qquad A(t) = \begin{bmatrix} -\frac{k}{2} \operatorname{sign}(\tilde{\eta}_v) Q_1(\tilde{\boldsymbol{q}}_v) & \frac{1}{2} Q_1(\tilde{\boldsymbol{q}}_v) I_v^{-1} R_v \\ \frac{\alpha}{2} \operatorname{sign}(\tilde{\eta}_v) R_v^T I_v^{-1} & 0 \end{bmatrix} \tag{18}$$

where the matrix $A(t)$ is known to be bounded for all $t \geq t_0$. Rewriting $\dot{V}(t)$ as $\dot{V}(t) = -\boldsymbol{x}(t)^T C^T C \boldsymbol{x}(t) \leq 0$, where

$$C = \begin{bmatrix} \sqrt{\frac{k}{2}} I_3 & 0 \end{bmatrix}$$

Theorem 4.5 and the discussion on pp. 626–628 in [10] show that the equilibrium point $\boldsymbol{x}(t) = 0$ of this well-defined, equivalent system is exponentially stable if the pair $(A(t), C)$ is uniformly completely observable (UCO). Because observability properties are unchanged under output feedback [10], $(A(t), C)$ are UCO if the pair $(A(t) - K(t)C, C)$ is uniformly observable for any piecewise continuous and bounded matrix $K(t)$, given that $A(t)$ is bounded [11]. Choose $K(t)$ as

$$K(t) = \begin{bmatrix} -\sqrt{k/2} \operatorname{sign}(\tilde{\eta}_v) Q_1(\tilde{\boldsymbol{q}}_v) \\ \sqrt{\alpha/2k} \operatorname{sign}(\tilde{\eta}_v) R_v^T I_v^{-1} \end{bmatrix}$$

$K(t)$ is bounded and is also piecewise continuous, based on the following properties. Note from the previous Lyapunov analysis that $\|\tilde{\boldsymbol{\varepsilon}}\| \to 0$. Because $\|\tilde{\boldsymbol{q}}_v\|^2 = 1 = \|\tilde{\boldsymbol{\varepsilon}}_v\|^2 + |\tilde{\eta}_v|^2$ for any time t, there exists a time $T > 0$ such that $|\tilde{\eta}_v| > 0$ for all $t > T$. Because $\tilde{\eta}_v$ therefore cannot pass through zero for $t > T$, $\operatorname{sign}(\tilde{\eta}_v)$ is constant for all $t > T$ and, hence, $K(t)$ is a piecewise continuous function of time.

The state transition matrix for the pair $(A(t) - K(t)C, C)$ is

$$\Phi(\tau, t) = \begin{bmatrix} I_3 & \Sigma(\tau, t) \\ 0 & I_3 \end{bmatrix} \tag{19}$$

where $\Sigma(\tau, t) = \frac{1}{2} \int_t^\tau Q_1[\tilde{\boldsymbol{q}}_v(\sigma)] I_v^{-1} R_v(\sigma)\, \mathrm{d}\sigma$, with $Q_1(\tilde{\boldsymbol{q}}_v)$ defined in Eq. (7). The observability gramian is then [12]

$$\begin{aligned} W(t, t+T) &= \int_t^{t+T} \Phi(\tau, t)^T C^T C \Phi(\tau, t)\, \mathrm{d}\tau \\ &= \int_t^{t+T} \begin{bmatrix} \frac{k}{2} I_3 & \frac{k}{2} \Sigma(\tau, t) \\ \frac{k}{2} \Sigma(\tau, t)^T & \frac{k}{2} \Sigma(\tau, t)^T \Sigma(\tau, t) \end{bmatrix} \mathrm{d}\tau \end{aligned} \tag{20}$$

The system is UCO if there exists a $T > 0$ and positive constants $\alpha_1 < \infty$, $\alpha_2 > 0$ such that, for all $t \geq t_0$, $\alpha_1 I \geq W(t, t+T) \geq \alpha_2 I$. Using lemma 13.4 of [10], this property is assured if $Q_1(\tilde{\boldsymbol{q}}_v) I_v^{-1} R_v$ and $\frac{\mathrm{d}}{\mathrm{d}t}(Q_1(\tilde{\boldsymbol{q}}_v) I_v^{-1} R_v)$ are bounded and there exist positive constants T_2, β_1, and a finite constant β_2 such that, for all $t \geq t_0$

$$\beta_2 I_3 \geq \int_t^{t+T_2} R_v^T I_v^{-1} Q_1(\tilde{\boldsymbol{q}}_v)^T Q_1(\tilde{\boldsymbol{q}}_v) I_v^{-1} R_v\, \mathrm{d}\tau \geq \beta_1 I_3 \tag{21}$$

$Q_1(\tilde{\boldsymbol{q}}_v) I_v^{-1} R_v$ is bounded, because all the signals in the estimator are bounded and the spacecraft inertia is bounded, hence the upper bound in (21) is satisfied. Substituting the equality $Q_1(\tilde{\boldsymbol{q}}_v)^T Q_1(\tilde{\boldsymbol{q}}_v) = I_3 - \tilde{\boldsymbol{\varepsilon}}_v \tilde{\boldsymbol{\varepsilon}}_v^T$ into Eq. (21) results in

$$\infty > \beta_2 I_3 \geq \int_t^{t+T_2} R_v^T I_v^{-1} \left(I_3 - \tilde{\boldsymbol{\varepsilon}}_v \tilde{\boldsymbol{\varepsilon}}_v^T \right) I_v^{-1} R_v\, \mathrm{d}\tau \geq \beta_1 I_3 > 0 \tag{22}$$

Recall that it has been shown that $\|\tilde{\boldsymbol{\varepsilon}}\| \to 0$ asymptotically. Thus, for any $\delta > 0$, there exists a $T_1(\delta) > t_0$ such that $\|\tilde{\boldsymbol{\varepsilon}}_v\| < \delta$ for all $t \geq t_0 + T_1$. Taking any $\delta < 1$, any $T_2 > T_1$, and any z in $\mathbb{R}^3$

$$\begin{aligned} \infty > (T_2 - T_1) \lambda_{\max}^2 \|z\|^2 &> z^T \left[\int_t^{t+T_2} \left(I - \tilde{\boldsymbol{\varepsilon}}_v \tilde{\boldsymbol{\varepsilon}}_v^T \right) \mathrm{d}\tau \right] z \\ &> (1 - \delta^2)(T_2 - T_1) \lambda_{\min}^2 \|z\|^2 > 0 \end{aligned} \tag{23}$$

where $\lambda_{\max}$ and $\lambda_{\min}$ are the maximum and minimum eigenvalues of I_v^{-1}. Finally $\frac{\mathrm{d}}{\mathrm{d}t}(Q_1(\tilde{\boldsymbol{q}}_v) I_v^{-1} R_v)$ is bounded, because all the terms in (15) are bounded. This demonstrates the required UCO property, and therefore $\tilde{\boldsymbol{\varepsilon}}_v$ and $\tilde{\boldsymbol{h}}_{i,v}$ approach zero exponentially fast (i.e., $\|\hat{\boldsymbol{\omega}}_v\| \to \|\boldsymbol{\omega}_v\|$ exponentially fast).

IV. Error Sources

The analysis provided in the previous section is for an ideal scenario. In reality, the measurements will be corrupted by errors. The primary error source considered here is the error in the relative attitude measurement used to derive the HST attitude quaternion. The resulting error in the HST attitude quaternion leads also to an error in the computation of the gravity gradient torque: the dominant external torque acting on the HST. The following analysis considers how the HST attitude error affects the estimator stability and convergence properties.

Denote by $\boldsymbol{q}_{v,m}$ the HST quaternion computed from a noisy measurement. Without loss of generality this term is assumed to have the form

$$\boldsymbol{q}_{v,m} = \boldsymbol{\delta q}_{\mathrm{err}} \otimes \boldsymbol{q}_v \tag{24}$$

where $\boldsymbol{\delta q}_{\mathrm{err}}$ is the error between the true HST quaternion $\boldsymbol{q}_v$ and $\boldsymbol{q}_{v,m}$. Similarly, the corresponding rotation matrices are given as $R_{v,m} = R(\boldsymbol{q}_{v,m}) = R(\boldsymbol{\delta q}_{\mathrm{err}}) R_v$. Post multiplying both sides of Eq. (24) by $\hat{\boldsymbol{q}}_v^{-1}$ gives $\tilde{\boldsymbol{q}}_{v,m} = \boldsymbol{\delta q}_{\mathrm{err}} \otimes \tilde{\boldsymbol{q}}_v$ and $R(\tilde{\boldsymbol{q}}_{v,m}) = R(\boldsymbol{\delta q}_{\mathrm{err}}) R(\tilde{\boldsymbol{q}}_v)$.

Because the true quaternion is unknown, Eqs. (13) and (14) cannot be implemented in the preceding estimator. Instead, $\boldsymbol{q}_{v,m}$ is used in place of $\boldsymbol{q}_v$, resulting in

$$\dot{\hat{\boldsymbol{q}}}_v = \tfrac{1}{2} Q(\hat{\boldsymbol{q}}_v) R(\tilde{\boldsymbol{q}}_{v,m})^T \left[I_v^{-1} R_{v,m} \hat{\boldsymbol{h}}_{i,v} + k \tilde{\boldsymbol{\varepsilon}}_{v,m} \operatorname{sign}(\tilde{\eta}_{v,m}) \right] \tag{25}$$

$$\dot{\hat{\boldsymbol{h}}}_{i,v} = \hat{T}_{i,v} + \tfrac{\alpha}{2} R_{v,m}^T I_v^{-1} \tilde{\boldsymbol{\varepsilon}}_{v,m} \operatorname{sign}(\tilde{\eta}_{v,m}) \tag{26}$$

$\hat{T}_{i,v}$ is the estimated external torque. The expressions for $R_{v,m}$ and $R(\tilde{\boldsymbol{q}}_{v,m})$ are substituted into (25)

$$\begin{aligned} \dot{\hat{\boldsymbol{q}}}_v = \tfrac{1}{2} Q(\hat{\boldsymbol{q}}_v) R(\tilde{\boldsymbol{q}}_v)^T \Big[& R(\boldsymbol{\delta q}_{\mathrm{err}})^T I_v^{-1} R(\boldsymbol{\delta q}_{\mathrm{err}}) R_v \hat{\boldsymbol{h}}_{i,v} \\ & + k R(\boldsymbol{\delta q}_{\mathrm{err}})^T \tilde{\boldsymbol{\varepsilon}}_{v,m} \operatorname{sign}(\tilde{\eta}_{v,m}) \Big] \end{aligned}$$

Rearranging the terms results in

$$\dot{\hat{\boldsymbol{q}}}_v = \tfrac{1}{2}Q(\hat{\boldsymbol{q}}_v)R(\tilde{\boldsymbol{q}}_v)^T\Big[I_v^{-1}R_v\hat{\boldsymbol{h}}_{i,v} + k\tilde{\boldsymbol{\varepsilon}}_v \operatorname{sign}(\tilde{\eta}_v) + \Delta_1\hat{\boldsymbol{h}}_{i,v} + \Delta_2\Big] \tag{27}$$

where

$$\Delta_1 = \Big[R(\delta\boldsymbol{q}_{\text{err}})^T I_v^{-1}R(\delta\boldsymbol{q}_{\text{err}}) - I_v^{-1}\Big]R_v$$

$$\Delta_2 = k[R(\delta\boldsymbol{q}_{\text{err}})^T\tilde{\boldsymbol{\varepsilon}}_{v,m}\operatorname{sign}(\tilde{\eta}_{v,m}) - \tilde{\boldsymbol{\varepsilon}}_v\operatorname{sign}(\tilde{\eta}_v)]$$

Δ_1 and Δ_2 are both bounded. Δ_1 results from the discrepancy in the HST inertia in the inertial frame due to the attitude measurement error. Δ_2 results directly from the attitude measurement error.

Next, Eq. (26) is analyzed. Recall that the true angular momentum is driven by the external torques acting on the HST, shown in Eq. (10). The dominant external torque acting on the HST is the gravity gradient torque. The gravity gradient torque in inertial coordinates is given as [13]

$$T_{i,v} = \frac{3\mu}{r_{i,v}^3}S\Big(\boldsymbol{r}_{i,v}^u\Big)R_v^T I_v R_v \boldsymbol{r}_{i,v}^u \tag{28}$$

where μ is the earth's gravitational parameter, $r_{i,v}$ is the magnitude of the HST inertial position vector, and $\boldsymbol{r}_{i,v}^u$ is the inertial position unit vector. The estimated torque in Eq. (26) is computed as

$$\hat{T}_{i,v} = \frac{3\mu}{r_{i,v}^3}S\Big(\boldsymbol{r}_{i,v}^u\Big)R_{v,m}^T I_v R_{v,m}\boldsymbol{r}_{i,v}^u \tag{29}$$

Substituting the expression for $R_{v,m}$ into (29), $\hat{T}_{i,v}$ is written as

$$\hat{T}_{i,v} = \frac{3\mu}{r_{i,v}^3}S\Big(\boldsymbol{r}_{i,v}^u\Big)R_v^T I_v R_v \boldsymbol{r}_{i,v}^u + \Delta_3 = T_{i,v} + \Delta_3 \tag{30}$$

$$\Delta_3 = \frac{3\mu}{r_{i,v}^3}S\Big(\boldsymbol{r}_{i,v}^u\Big)\Big[R_{v,m}^T I_v R_{v,m} - R_v^T I_v R_v\Big]\boldsymbol{r}_{i,v}^u$$

Substituting (30) and $R_{v,m}$ into (26) results in

$$\dot{\hat{\boldsymbol{h}}}_{i,v} = T_{i,v} + \Delta_3 + \tfrac{\alpha}{2}R_v^T I_v^{-1}\tilde{\boldsymbol{\varepsilon}}_v\operatorname{sign}(\tilde{\eta}_v) + \Delta_4 \tag{31}$$

where

$$\Delta_4 = \tfrac{\alpha}{2}R_v^T\Big[R(\delta\boldsymbol{q}_{\text{err}})^T I_v^{-1}\tilde{\boldsymbol{\varepsilon}}_{v,m}\operatorname{sign}(\tilde{\eta}_{v,m}) - I_v^{-1}\tilde{\boldsymbol{\varepsilon}}_v\operatorname{sign}(\tilde{\eta}_v)\Big]$$

Combining Eqs. (27) and (31) with (11) and (10), we get

$$\begin{bmatrix}\dot{\tilde{\boldsymbol{q}}}_{v,m}\\ \dot{\tilde{\boldsymbol{h}}}_{i,v}\end{bmatrix} = \begin{bmatrix}\tfrac{1}{2}Q(\tilde{\boldsymbol{q}}_v)\Big[I_v^{-1}R_v\tilde{\boldsymbol{h}}_{i,v} - k\tilde{\boldsymbol{\varepsilon}}_v\operatorname{sign}(\tilde{\eta}_v)\Big] + \Delta_1'\hat{\boldsymbol{h}}_{i,v} + \Delta_2'\\ -\tfrac{\alpha}{2}R_v^T I_v^{-1}\tilde{\boldsymbol{\varepsilon}}_v\operatorname{sign}(\tilde{\eta}_v) + \Delta_3' + \Delta_4'\end{bmatrix} \tag{32}$$

where $\Delta_1' = -\frac{1}{2}Q(\tilde{\boldsymbol{q}}_v)\Delta_1$, $\Delta_2' = -\frac{1}{2}Q(\tilde{\boldsymbol{q}}_v)\Delta_2$, $\Delta_3' = -\Delta_3$, and $\Delta_4' = -\Delta_4$.

Equation (32) has the form

$$\dot{\boldsymbol{x}}(t) = \boldsymbol{f}(\boldsymbol{x},t) + \boldsymbol{d}(\boldsymbol{x},t)$$

where $\boldsymbol{f}(\boldsymbol{x},t)$ has been shown to be exponentially stable and

$$\boldsymbol{d}(t) = \begin{bmatrix}\Delta_1'\hat{\boldsymbol{h}}_{i,v} + \Delta_2'\\ \Delta_3' + \Delta_4'\end{bmatrix} = \boldsymbol{d}_1(t) + \boldsymbol{d}_2(t)$$

where

$$\boldsymbol{d}_1(t) = \begin{bmatrix}\Delta_1'\hat{\boldsymbol{h}}_{i,v}\\ 0\end{bmatrix}$$

and $\boldsymbol{d}_2(t)$ contains the remaining terms, which are all bounded. Because $\boldsymbol{d}_2(t)$ is bounded, the exponentially stable system is robust to this perturbation. The concern, however, is with $\boldsymbol{d}_1(t)$, which contains part of the state and hence cannot be assumed bounded a priori. If exponential stability is preserved with $\boldsymbol{d}_1(t)$, then the system will be robust to the combined disturbance $\boldsymbol{d}(t)$.

Since perturbation $\boldsymbol{d}_1(t)$ can be bounded by a constant times the norm of the state, and the nominal system is exponentially stable, [10] (Lemma 5.2) shows that exponential stability is preserved if the magnitude of Δ_1' is sufficiently small. In the general case where Δ_1' is larger, the potential instability resulting from $\boldsymbol{d}_1(t)$ can be removed through a minor modification of the estimator. This is accomplished by introducing a "leakage" term [11] in Eq. (26).

$$\dot{\hat{\boldsymbol{h}}}_{i,v} = \hat{T}_{i,v} + \tfrac{\alpha}{2}R_{v,m}^T I_v^{-1}\tilde{\boldsymbol{\varepsilon}}_{v,m}\operatorname{sign}(\tilde{\eta}_{v,m}) - \sigma(\hat{\boldsymbol{h}}_{i,v})\hat{\boldsymbol{h}}_{i,v} \tag{33}$$

where

$$\sigma(\hat{\boldsymbol{h}}_{i,v}) = \begin{cases}\sigma_o & \text{if } \|\hat{\boldsymbol{h}}_{i,v}\| > \|\boldsymbol{h}_{i,v}\|_{\max} > \|\boldsymbol{h}_{i,v}\|\\ 0 & \text{otherwise}\end{cases}$$

where the scalar $\sigma_o > 0$ and $\|\boldsymbol{h}_{i,v}\|_{\max}$ is a known upper bound on the HST angular momentum (established by analyzing the pure tumbling scenario). This modification serves to force the magnitude of the angular momentum estimate to decrease if ever it exceeds a known prior bound on the feasible magnitude of the actual HST momentum. The effectiveness of the leakage term is demonstrated by considering how the additional term in (33) enters a Lyapunov analysis:

$$\sigma\tilde{\boldsymbol{h}}_{i,v}^T\hat{\boldsymbol{h}}_{i,v} = \sigma\tilde{\boldsymbol{h}}_{i,v}^T(\boldsymbol{h}_{i,v} - \tilde{\boldsymbol{h}}_{i,v}) = -\sigma\|\tilde{\boldsymbol{h}}_{i,v}\|^2 + \sigma\tilde{\boldsymbol{h}}_{i,v}^T\boldsymbol{h}_{i,v}$$

Applying Young's inequality results in

$$\sigma\tilde{\boldsymbol{h}}_{i,v}^T\hat{\boldsymbol{h}}_{i,v} \le -\tfrac{1}{2}\sigma\|\tilde{\boldsymbol{h}}_{i,v}\|^2 + \tfrac{1}{2}\sigma\|\boldsymbol{h}_{i,v}\|^2$$

Because $\boldsymbol{h}_{i,v}$ is assumed to be bounded, the second term acts as another bounded disturbance, which can be combined with $\boldsymbol{d}_2$. The first term, however, acts to stabilize the possible high noise instability identified previously. The added terms in the Lyapunov analysis ensure that the leakage modification preserves the exponential stability of the estimator dynamics in the presence of the disturbance term $\boldsymbol{d}_2$ and thus guarantees that the estimation errors will exponentially converge to below a bound determined by $\|\boldsymbol{d}_2\|$. If there are no measurement errors, $\|\boldsymbol{d}_1\| = 0$ and the estimator converges to the true angular velocity, as in the previous section.

Although it looks like this technique adds an additional disturbance, possibly stabilizing the system but adding extra error sources, in fact, this is not the case. Expanding the added term instead as

$$\sigma\tilde{\boldsymbol{h}}_{i,v}^T\hat{\boldsymbol{h}}_{i,v} = \sigma(\boldsymbol{h}_{i,v} - \hat{\boldsymbol{h}}_{i,v})^T\hat{\boldsymbol{h}}_{i,v} = \sigma\boldsymbol{h}_{i,v}^T\hat{\boldsymbol{h}}_{i,v} - \sigma\|\hat{\boldsymbol{h}}_{i,v}\|^2$$

or

$$\sigma\tilde{\boldsymbol{h}}_{i,v}^T\hat{\boldsymbol{h}}_{i,v} \le \tfrac{1}{2}\sigma[\|\boldsymbol{h}_{i,v}\|^2 - \|\hat{\boldsymbol{h}}_{i,v}\|^2]$$

Recall from Eq. (33) that $\sigma > 0$ only if $\|\hat{\boldsymbol{h}}_{i,v}\| > \|\boldsymbol{h}_{i,v}\|$. Thus the added term is always negative; essentially the extra constraint in the estimation law for the angular momentum can only help convergence. Note that if the size of the perturbation due to the measurement errors is sufficiently large to require use of leakage to stabilize the algorithm, the resulting RMS prediction errors are likely to be quite poor. Because the leakage can only improve the convergence, however, it is a useful safety feature to include in the algorithm, regardless of the noise level.

V. Simulation Results

The algorithm outlined in the previous sections is tested with a simulation. The simulation includes two orbits of data based on an actual HST ephemeris. The HST inertia is [14]

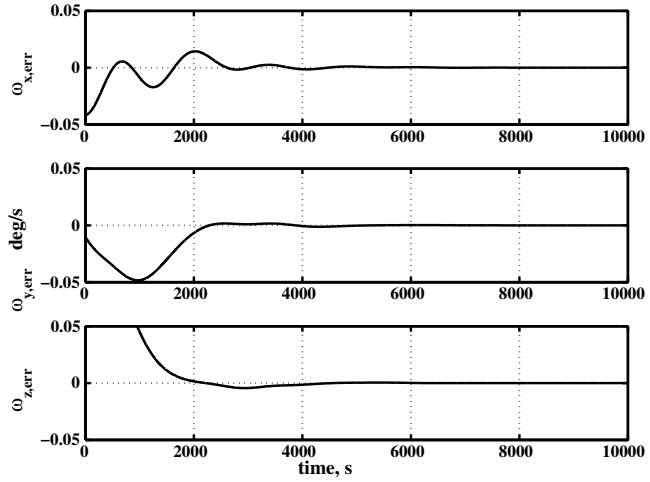

Fig. 1 Angular velocity errors, no attitude measurement error.

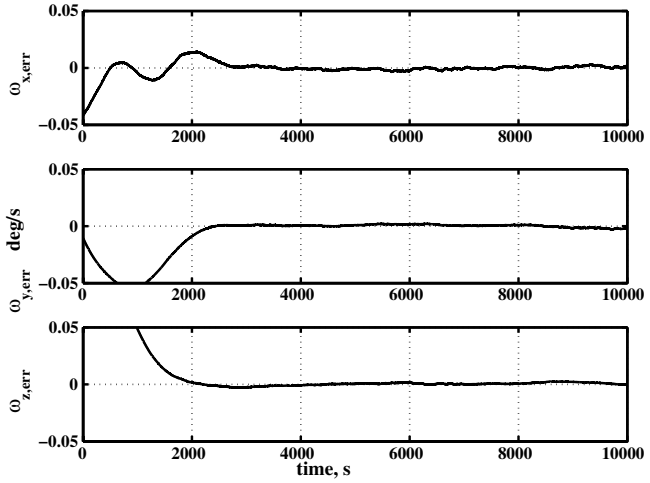

Fig. 2 Angular velocity errors, random 15-deg measurement error.

$$I_v = \begin{bmatrix} 36,046 & -706 & 1491 \\ -706 & 86,868 & 449 \\ 1491 & 449 & 93,848 \end{bmatrix} \text{ kg} \cdot \text{m}^2$$

The algorithm is initially tested without any errors. The initial attitude quaternion is identity $\boldsymbol{q}_v = \hat{\boldsymbol{q}}_v = [0, 0, 0, 1]$. The initial HST angular velocity estimate is zero, $\hat{\boldsymbol{\omega}}_v = [0, 0, 0]$, and the true initial angular velocity is $\boldsymbol{\omega}_v = [-0.04, -0.01, 0.14]$ deg /s. The gains are chosen as $k = 0.005$ and $\alpha = 90,000$. In all cases, the estimator is run at 2 Hz. Next, attitude measurement errors are introduced by rotating each true relative attitude measurement by a random angle about a random direction. The random angle is generated from a zero mean, normal distribution with a standard deviation of 15 deg. The random direction is generated from a zero mean, uniform distribution.

Figure 1 is an example of the resulting angular velocity error from the nonlinear estimator with no attitude measurement errors. Figure 2 is a sample of the angular velocity error with erroneous measured attitudes. Next, 100 test cases are run, and each case has a different sample of erroneous measured attitudes. Table 1 lists the average of the final RMS angular velocity error for each of the 100 test cases.

Table 1 Average final rms angular velocity errors

Angular velocity error component	Average, deg/s
$\tilde{\omega}_{x,\text{RMS}}$	0.00164
$\tilde{\omega}_{y,\text{RMS}}$	0.00164
$\tilde{\omega}_{z,\text{RMS}}$	0.00127

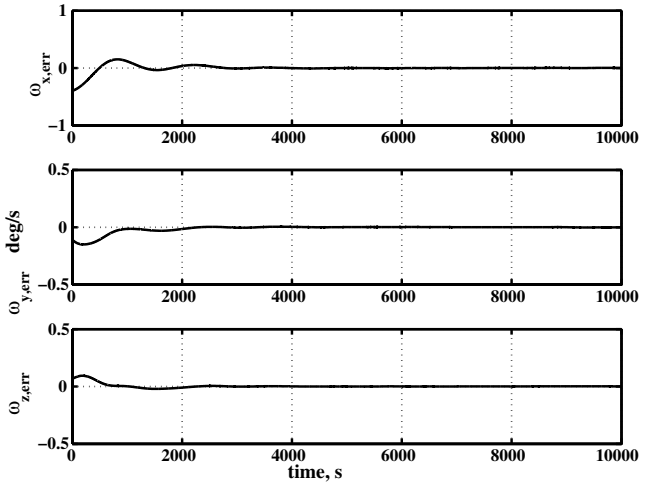

a) Nonlinear with leakage

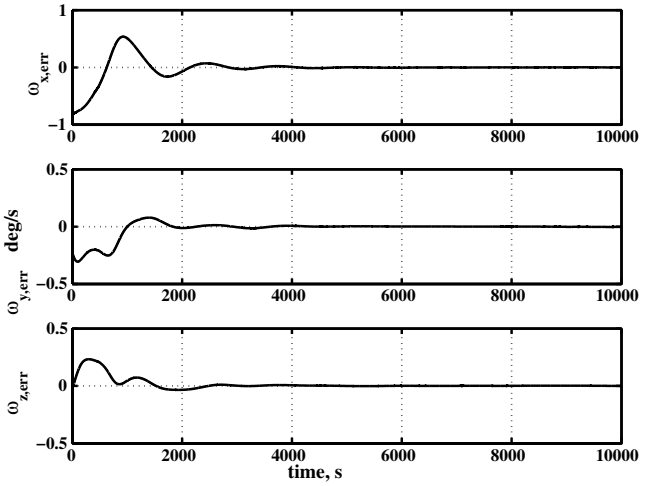

b) Nonlinear without leakage

Fig. 3 Angular velocity errors, large initial angular velocity estimate.

Next, the leakage term of Eq. (33) is added to the nonlinear estimator, with $\sigma_o = 1$. To see the improvement in the estimation, the initial angular velocity estimate is increased such that the initial angular momentum estimate exceeds the maximum anticipated angular momentum. Figure 3a shows the angular velocity errors with the leakage term, and 3b shows the same scenario without the leakage term. In both cases, the nonlinear estimator converges; however, the additional term does improve the convergence time.

VI. Conclusion

A nonlinear algorithm is developed to estimate the rotation rates for a noncooperative target vehicle. The nonlinear algorithm determines the rotation rate through an estimation of the inertial angular momentum. The algorithm, designed for the Hubble robotic servicing mission, applies in particular to the scenario in which the batteries have died and the HST is tumbling. The HRV design includes vision and feature-recognition sensors capable of producing a relative attitude quaternion. Combining the relative attitude with the HRV inertial attitude produces the measured HST attitude for the estimation algorithm.

Simulation results are presented for two orbits of HST data. The nonlinear algorithm is tested first with perfect data, and then the measured attitude is corrupted with random attitude errors with an uncertainty of 15 deg. The results from 100 test cases, with different random measured attitudes in each case, are presented. In all cases, the nonlinear estimator converges and estimates the HST angular velocity.

Future work will focus on improving the accuracy of the relative attitude quaternion computed from the vision and feature recognition sensors. For the HST robotic repair mission, the primary error source was the uncertainty in the measured attitude. The HST inertia properties have been analyzed extensively and are not considered to be a significant source of error. However, uncertainties in the spacecraft inertia should be addressed in future studies for other missions, as well as a more rigorous study of the nonlinear estimator gains. Also, the algorithms will be coupled with a control scheme to study the closed loop behavior during a rendezvous or docking scenario.

Acknowledgments

The authors would like to thank John VanEepoel and Steve Queen of the NASA Goddard Space Flight Center for their contributions to this work.

References

[1] Salcudean, S., "A Globally Convergent Angular Velocity Observer for Rigid Body Motion," *IEEE Transactions on Automatic Control*, Vol. 36, No. 12, Dec. 1991, pp. 1493–1496.

[2] Vik, B., Shiriaev, A., and Fossen, T. I., "Nonlinear Observer Design for Integration of DGPS and INS," *New Directions in Nonlinear Observer Design*, Springer–Verlag, Berlin, 1999.

[3] Thienel, J., and Sanner, R. M., "A Coupled Nonlinear Spacecraft Attitude Controller and Observer with an Unknown Constant Gyro Bias and Gyro Noise," *IEEE Transactions on Automatic Control*, Vol. 48, No. 11, Nov. 2003, pp. 2011–2015.

[4] Thienel, J., "Nonlinear Observer/Controller Designs for Spacecraft Attitude Control Systems with Uncalibrated Gyros," Ph.D. Thesis, Univ. of Maryland, College Park, MD, 2004.

[5] Shuster, M. D., "A Survey of Attitude Representations," *The Journal of Astronautical Sciences*, Vol. 41, No. 4, Oct.–Dec. 1993, pp. 439–517.

[6] Sanner, R. M., "Adaptive Attitude Control Using Fixed and Dynamically Structured Neural Networks," AIAA Paper 96–3891, 1996.

[7] Wie, B., *Space Vehicle Dynamics and Control*, AIAA Education Series, AIAA, Reston, VA, 1998.

[8] Krstić, M., Kanellakopoulos, I., and Kokotovic, P., *Nonlinear and Adaptive Control Design*, Wiley, New York, 1995.

[9] Slotine, J.-J. E., and Li, W., *Applied Nonlinear Control*, Prentice–Hall, Upper Saddle River, NJ, 1991.

[10] Khalil, H. K., *Nonlinear Systems*, 2nd ed., Prentice–Hall, Upper Saddle River, NJ, 1996.

[11] Ioannou, P., and Sun, J., *Robust Adaptive Control*, Prentice–Hall, Upper Saddle River, NJ, 1995.

[12] Chen, C.-T., *Linear System Theory and Design*, 2nd ed., Oxford Univ. Press, Oxford, 1984.

[13] Wertz, J. R. (ed.), *Spacecraft Attitude Determination and Control*, D. Reidel Publishing, Dordrecht, The Netherlands, 1984.

[14] Queen, S., "HRV GNC Peer Review, Flight Performance Analysis," [internal NASA report], NASA 2004.